Non-canonical Hedgehog signaling through L-type voltage gated Ca^{2+} channels controls CD8$^+$ T cell killing

Joachim Hanna, Chrysa Kapeni, Louise O'Brien, Valentina Carbonaro, Flavio Beke, Chandra Chilamakuri, and Maike de la Roche[§]

University of Cambridge, Cancer Research UK Cambridge Institute, Robinson Way, Cambridge CB2 0RE, UK

[§]Corresponding author. Email: maike.delaroche@cruk.cam.ac.uk (M.d.l.R.)

ABSTRACT

Cytotoxic CD8$^+$ T lymphocytes (CTLs) are critical to the immune response against intracellular pathogens and cancer and act by eliminating infected and malignant cells through targeted secretion of cytotoxic granules. Hedgehog (Hh) signaling has been shown to be critical for CTL killing. Interestingly, Hh signaling in CD8$^+$ T cells is not induced by extracellular Hh ligands but is initiated upon T cell receptor (TCR) engagement. How the TCR induces the Hh pathway independently of extracellular Hh ligands is unknown. Here we show that the Hh transcription factor Gli1 is essential for efficient CTL function and is induced downstream of the TCR by an extracellular Ca^{2+} influx selectively controlled by L-type voltage gated Ca^{2+} channels localized at the plasma membrane. We demonstrate that this novel mode of Hh signaling induction is independent of the canonical Hh pathway and represents the primary mechanism of Gli1 induction in naïve CD8$^+$ T cells, while CTLs can also activate Gli1 via MAP Kinase signaling. Importantly, we show that this L-type voltage gated Ca^{2+} channel-controlled Gli1 induction is functionally required for CTL killing in mice and humans. Gli inhibitors are currently in clinical trials against various cancers and our observations indicate that they likely inhibit the anti-tumor response.

1

Significance statement

Cytotoxic CD8$^+$ T cells (CTLs) kill infected and malignant cells by targeted secretion of cytotoxic granules. Hedgehog signaling is critical for effective CTL killing and is activated by the T cell receptor (TCR) independently of exogenous Hedgehog ligands. This study shows that Hedgehog transcription factor Gli1 is required for CTL killing and identifies L-type voltage gated Ca^{2+} channels (Ca$_v$1) as essential regulators of CTL killing in mouse and human, by virtue of their ability to activate Gli1 downstream of the TCR. This Ca$_v$1-Gli1 axis operates independently of canonical Hedgehog signaling. Our work suggests that caution is required when using Gli inhibitors, currently in trials as anti-cancer therapeutics, since they may dampen the anti-tumor response.

INTRODUCTION

Cytotoxic CD8$^+$ T lymphocytes (CTLs) eradicate infected and cancerous cells by targeted release of cytotoxic granules. Two types of immune synapses are important for this to occur: the signaling and the cytotoxic synapse. The signaling synapse initiates CTL differentiation and is formed between a naïve CD8$^+$ T cell and an antigen presenting cell (APC). The cytotoxic synapse is formed between a CTL and its target cell whereby engagement of the TCR initiates the secretion of granules containing cytotoxic perforin and granzyme. Both synapses promote optimal TCR signaling [1].

Immune synapses are structurally and functionally very similar to the primary cilium, a hairlike protrusion from the cell body present on most cells. For example, both structures dock the centrosome at the plasma membrane via distal appendage proteins and are key signaling hubs and sites of focussed endo- and exocytosis [1, 2]. The similarities between immune synapses and primary cilia prompted us to study Hedgehog (Hh) signaling – a pathway functionally tied to the primary cilium in vertebrates – at the T cell synapse.

Canonical Hh signaling is initiated when one of three Hh ligands - Sonic Hh (Shh), Indian Hh (Ihh) or Desert Hh (Dhh) - bind to the transmembrane receptor Ptch at the base of the primary cilium. Upon ligand binding, Ptch releases its inhibition of the key signal

2

transducer Smo that translocates to the cilium and activates glioma associated oncogene (Gli) transcription factors (Gli1, Gli2, and Gli3). Gli transcription factors translocate into the nucleus and initiate Hh target gene transcription [3]. More recently, however, various non-canonical Hh signaling modes have been described which can be divided into two major groups. The first group is independent of Gli transcription: Ptch can act as a dependence receptor and triggers apoptosis in the absence of Hh ligands [4], and Smo can regulate the actin cytoskeleton via small GTPases RhoA and Rac1 which occurs through G-proteins and PI3K in fibroblasts and through Src and Fyn in neurons [5, 6]. Smo can also trigger calcium (Ca^{2+}) release from the endoplasmic reticulum (ER) and in spinal neurons through G_i protein and PLCγ-catalysed generation of IP_3 and the opening of IP_3-dependent channels [7]. The second group is Gli transcription-dependent and Ptch/Smo-independent. This non-canonical activation of Gli1 has been described in cancers and stem cells [8]. Positive regulators include the MAP Kinase (MAPK) pathway, PI3K-AKT-mTOR, and TGFβ signaling as well as oncogenes such as c-myc.

Although various roles for Hh signaling during T cell development in the thymus have been proposed [9], little is known about Hh signaling in mature T cells. We have previously shown that Hh signaling is necessary for CD8^{+} T cell killing and, interestingly, is initiated independently of extracellular Hh ligands [10]. We previously demonstrated that proximal TCR signaling is the main inducer of the Hh pathway [10] but the mechanism by which Hh signaling is initiated downstream of the TCR remains unknown.

Gli1 is the only Gli transcription factor expressed in CD8^{+} T cells. Here we show that Gli1 is critical for CD8^{+} T cell killing. We demonstrate a key role for MAPK signaling inducing Gli1 in CTLs, as has been previously described in other cell types and tumor cells [11]. Additionally, we find binding sites of the MAPK induced transcription factor activator protein 1 (AP-1) in the Gli1 promoter. Most importantly, we identify a previously unknown, non-canonical mode of Hh signaling that culminates in Gli activation via L-type voltage gated Ca^{2+} channels (Ca_v1 family) in both CTLs and naïve CD8^{+} T cells.

Published work has shown that constitutive loss of Ca_v1 channels in all tissues leads to defects in T cell development and maturation, with subsequent functional impairment of peripheral T cells [12, 13]. However, it is not fully clear what cell-intrinsic role these channels

3

95 play in fully mature T cells. Our work demonstrates that Ca_v1 channels are critical for mature $CD8^+$ T cell killing by virtue of their ability to induce Gli1 via non-canonical Hh signaling.

RESULTS

100

Gli1 is important for cytotoxic T cell (CTL) killing

Gli1 is the only Gli transcription factor reported to be present in $CD8^+$ T cells [10] and functions as a reliable marker of Hh signaling activation [14]. Previous work has shown that CTLs treated with the small molecule Gli inhibitor GANT61 have diminished killing ability
105 [10]. We wanted to confirm this observation genetically and generated $Gli1^{eGFP/eGFP}$ ($Gli1$ KO) by breeding $Gli1^{eGFP/+}$ mice to homozygosity, disrupting the expression of the $Gli1$ gene. $Gli1$ KO mice have a phenotypically normal peripheral T cell compartment (Suppl. Fig. 1) and $CD8^+$ T cells from the $Gli1$ KO mice lack Gli1 protein (Fig. 1A). $CD8^+$ T cells from OTI TCR transgenic mice recognize ovalbumin (Ova) peptide residues 257-264 in
110 the context of MHCI $H2K^b$ and we bred $Gli1$ KO mice expressing the OTI TCR. We compared $Gli1$ WT and KO OTI cells in their ability to kill Ova-presenting EL-4 murine lymphoma target cells. Strikingly, specific T cell killing was reduced by 25-50% in the $Gli1$ KO cells compared with the $Gli1$ WT controls (Fig. 1B). Thus, Gli1 is functionally important for effective CTL killing.

115

MAP kinase signaling downstream of the TCR promotes Gli1 induction in CTLs

$CD8^+$ T cell killing is initiated by engagement of the TCR and the TCR-associated proximal tyrosine kinase Lck has been shown to be required for the induction of Gli1 [10]. Induction
120 of $Gli1$ mRNA is a robust readout of Gli1 activation and thus active Hh signalling [14]. We therefore wanted to investigate how signaling downstream of the TCR leads to Gli1 activation.

TCR engagement by cognate antigen presented on MHCI molecules leads to recruitment of Lck to the TCR complex (Fig. 2A). Lck phosphorylates ZAP70 (ζ-chain-associated

4

125   protein kinase of 70 kDa) which in turn phosphorylates the adaptor protein LAT (Linker for activation of T cells) leading to the formation of the LAT signalosome. The LAT signalosome propagates signal branching into three major signaling pathways ultimately culminating in the activation of the transcription factors NFAT, NFκB, and AP-1 [15].

The three signaling branches of the TCR: NFAT, NF-κB, and AP-1, respectively, can be
130   pharmacologically manipulated. Ionomycin is a Ca^{2+} ionophore that increases cytosolic Ca^{2+} via release of Ca^{2+} from ER stores, leading to activation of NFAT. Phorbol 12-myristate 13-acetate (PMA) activates PKCs and thus NFκB and AP-1 transcription factors. When naïve $CD8^+$ T cells or CTLs were treated with both PMA and Ionomycin, to achieve maximum activation of the T cells, *Gli1* RNA was induced 30 and 3-fold,
135   respectively (Fig. 2B). On their own however, only PMA induced significant upregulation of Gli1 in naïve T cells and CTLs, while ionomycin had only a small effect on Gli1 levels at the highest concentration. This suggested that NFAT signaling might be less important in Gli1 induction.

Since mimicking TCR engagement by PMA and Ionomycin is not physiological, we
140   decided to specifically block the three branches of TCR signaling downstream of TCR crosslinking.

The NFAT and NFκB signaling branches can be specifically blocked by transfecting primary $CD8^+$ T cells with VIVIT or Dominant Negative (DN)IkBα, respectively. VIVIT is a 16mer peptide that selectively disrupts the interface between Calcineurin and NFAT [16].
145   As expected, VIVIT-expressing CTLs showed reduced IL-2 and IFNγ production (Suppl. Fig. 2A). DN IkBα cannot be phosphorylated by IKKβ and thus NFκB is sequestered in the cytosol [17]. Indeed, CTLs transfected with DN IkBα had reduced nuclear NFκB translocation (Suppl. Fig. 2B). When Gli1 induction was assessed at steady state and after 3 hours of restimulation, VIVIT- and DN IkBα -expressing CTLs had no defect in Gli1
150   induction compared to GFP-transfected controls (Fig. 2C).

The third branch of TCR signaling leading to AP-1 activation can be blocked by U0126, a selective MAP Kinase (MEK1 and MEK2) inhibitor (Suppl. Fig. 2C) [18]. U0126 treatment did not affect cell viability (Suppl. Fig. 3A), but led to a significant reduction of Gli1 induction after TCR stimulation in CTLs and to a much lesser degree in naïve $CD8^+$ T
155   cells (Fig. 2D). MAPK signaling has been shown to be able to activate Gli1 through one

5

of two mechanisms. The first is through direct activation of Gli1 transcription by AP-1 heterodimer which is formed by one Fos and one Jun (c-Jun, JunB or JunD) family member. The second mechanism is via the kinase activity of MAPK which activates an unknown upstream regulator of Gli1 [11].

160

To determine which mode of MAPK signaling is responsible for the Gli1 induction, we reanalysed existing ChIP-Seq datasets generated by *Kurachi et al.* to assess direct AP-1 binding to genomic locus of Gli1 in CTLs [19]. Since AP-1 has been demonstrated to bind upstream of the *Ifng* locus [20, 21], we analysed whether Jun transcription factors bind to this

165 locus in the dataset, and indeed, all three Jun family members bind upstream of the *Ifng* locus (Fig. 2E, top panel). Interestingly, we observed that both c-Jun and JunB also bind upstream of the *Gli1* locus (Fig. 2E). By contrast, no binding was observed upstream of the *Gli2* and the *Gli3* loci, which are both not expressed in CTLs [10] (Fig. 2E).

Taken together, this data indicates that of the main downstream signaling arms of the

170 TCR (NFAT, NF-κB, AP-1), AP-1 signaling selectively controls Gli1 induction in CTLs, in part by direct binding of AP-1 to the genomic locus of *Gli1*. However, none of the major downstream signaling arms appear to be individually responsible for Gli1 induction in naïve CD8$^+$ T cells.

175 **Ca^{2+} is required for Gli1 induction**

We could not clearly associate the induction of Gli1 with one specific branch of TCR signaling in naïve CD8$^+$ T cells. While MAPK signaling accounted to some extent for the induction of Gli1 in CTLs, it was still not clear what other pathways drive the induction of Gli1 in CD8$^+$ T cells. Ca^{2+} is required for the initiation of canonical Hh signaling at the level

180 of the Ihh:Ptch interaction [22] and is an important second messenger in T cells [23]. We therefore investigated whether Ca^{2+} signaling was important for Gli1 induction. We subjected naïve T cells and CTLs to treatment with a cell-permeable high-affinity Ca^{2+} chelator, BAPTA-AM, prior to TCR stimulation. Ca^{2+} chelation with BAPTA-AM led to complete abrogation of Gli1 induction in naïve T cells and a significant reduction of *Gli1*

185   mRNA and protein induction in CTLs upon TCR stimulation (Fig. 3A). BAPTA-AM can chelate Ca^{2+} in both intra- and extracellular compartments. To determine the relative contribution of each of these pools of Ca^{2+} to Gli1 induction, we repeated the experiments using non-cell-permeable BAPTA or EGTA which both chelate extracellular Ca^{2+}. Extracellular Ca^{2+} chelation significantly reduced Gli1 induction in CTLs (Fig. 3B). Thus,

190   Ca^{2+} signaling is essential for Gli1 induction and relies on both extra- and intracellular Ca^{2+} pools.

L-type voltage gated Ca^{2+} channels are critical for Gli1 induction and act independently of MAPK signaling

195   We next sought to determine whether Ca^{2+} signaling through a specific Ca^{2+} channel is responsible for regulating Gli1 induction. We targeted channels previously shown to be expressed in T cells such as CRAC channels, L-type voltage-gated Ca^{2+} channels (Ca_v1), TRPV, TRPA and P2X channels with small-molecule inhibitors (Fig. 3C) [23]. Treatment of CTLs with small molecule inhibitors at doses previously published in the literature had no

200   effect on cell viability during the course of the experiment (Suppl. Fig. 3A). Interestingly, inhibition of CRAC channels showed no effect on Gli1 induction and neither did inhibition of TRPV, TRPA and P2X channels.

     Only inhibition of Ca_v1 channels with Nifedipine showed a dose-dependent reduction of Gli1 induction in CTLs (Fig. 3D). Ca_v1 channels have been shown to play a critical role in

205      $CD8^+$ T cell development [24]. Evidence in the literature has shown that constitutive knockout of *CACNA1F* (encoding $Ca_v1.4$) during T cell development results in impaired MAPK signaling strength [12]. We hence sought to determine whether the effect of Nifedipine on Gli1 induction in CTLs was through inhibition of MAPK signaling or through an independent mechanism. Inhibition of both, MAPK and Ca_v1 channels, showed an

210   additive decrease in Gli1 induction (Fig. 3D) but importantly pErk levels were unaffected by treatment with Nifedipine (Fig. 3E), indicating that Ca_v1 channels were regulating Gli1 induction through a mechanism distinct from MAPK signaling. Given that MAPK signaling is not a major driver of Gli1 induction in naïve $CD8^+$ T cells (Fig. 2D) we sought to

7

215   investigate whether Ca_v1 channels might be the main source of Gli1 induction. Nifedipine treatment of naïve CD8$^+$ T cells resulted in complete abrogation of Gli1 induction post TCR stimulation (Fig. 3F).

We wanted to confirm this finding by genetic ablation of Ca_v1 channels and performed CRISPR knockouts of each of the known Ca_v1 α_1 subunit coding genes (*CACNA1S/C/D/F*) in primary murine CD8$^+$ T cells. Knockout of individual genes did not

220   show a significant decrease in Gli1 induction (Suppl. Fig. 4A) indicating that there may be a degree of redundancy between individual Ca_v1 family channels. $Ca_v1.3$ and 1.4 KO led to the most sustained reduction in Gli1 induction. Thus, we next performed a double knockout of *CACNA1D and CACNA1F*, which encode $Ca_v1.3$ and $Ca_v1.4$, respectively. The double knockouts showed high knockout efficiency (Suppl. Fig. 4B) and normal cell

225   proliferation (Suppl. Fig. 4C). T cells double knockout for $Ca_v1.3$ and $Ca_v1.4$ had intact MAPK signaling (Fig. 3G) but a striking inability to induce Gli1 upon stimulation (Fig. 3H).

Thus, we have shown that Ca_v1 channels are the main inducers of Gli1 in naïve CD8$^+$ T cells and in CTLs act together with MAPK signaling to induce Gli1.

230   **Ca_v channels localize to the plasma membrane and intracellular vesicles in human CD8$^+$ T cells and are important for killing**

To interrogate whether Ca_v1 channels are also expressed in human CD8$^+$ T cells we profiled the expression of Ca_v1 α_1 subunit coding genes (CACNA1S/C/D/F corresponding to $Ca_v1.1$, $Ca_v1.2$, $Ca_v1.3$, and $Ca_v1.4$, respectively) in naïve CD8$^+$ T cells from multiple

235   healthy donors (Fig. 4A). While $Ca_v1.1$ and $Ca_v1.2$ were not expressed in human CD8$^+$ T cells, we readily detected expression of $Ca_v1.3$ and $Ca_v1.4$, the two subunits responsible for Gli1 induction in murine T cells with $Ca_v1.4$ being 50-fold higher expressed than $Ca_v1.3$.

Next, we wanted to know whether the Ca_v1 channel inhibitor Nifedipine could block GLI1

240   induction in human CD8$^+$ T cells as it did in murine cells (Fig. 3F). The concentration of

8

Nifedipine used had no effect on cell viability (Suppl. Fig. 3B) but induction of GLI1 was ablated in Nifedipine-treated human CD8+ T cells (Fig. 4B).

Ca$_v$1 channels have been hypothesized to localize to the plasma membrane in T cells [12] but have never been localized by immunofluorescence. Using an antibody against Ca$_v$1.4 [25], we stained human CD8+ T cells from different healthy donors and consistently observed specific staining at the plasma membrane as well as on intracellular vesicles in all donors (Fig. 4C).

To investigate whether Ca$_v$1 channels are implicated in the ability of human CD8+ T cells to kill tumor targets, we treated human CTLs from various donors with Nifedipine or carrier control before subjecting them to a killing assay. While carrier-treated human CTLs were able to kill tumor targets, Nifedipine-treated CTLs from all donors tested showed a marked decrease in killing ability (Fig. 4D).

Taken together, we have shown that, similarly to murine CD8+ T cells, human CD8+ T cells express Ca$_v$1 channels and depend on them for GLI1 upregulation and consequent target cell killing.

L-type voltage gated Ca^{2+} channels regulate T cell killing in a Gli1-dependent manner

To definitively answer whether the effect of Ca$_v$1 channel blockade via Nifedipine on CTL killing is achieved through Gli1 or an independent mechanism, we treated *Gli1* WT and *Gli1* KO CTLs with Nifedipine or carrier control (Fig. 5A). We find that Nifedipine treatment leads to a defect in killing in *Gli1* WT CTLs, which we have shown to be independent of effects on cell viability or MAPK signaling (Fig. 3E, Suppl. Fig. 3A). This indicates that Ca$_v$1 channels are important regulators of CTL killing. Treatment of *Gli1* KO CTLs with Nifedipine showed no additive defect in killing compared to carrier control (Fig. 5A), indicating that the presence of Gli1 is required for Nifedipine to exert its effect on CTL killing.

Thus, we have shown that L-type voltage gated Ca^{2+} channels are critical for CTL killing and that the mechanism for this killing phenotype is by regulating the induction of Gli1.

270

Gli1 induction upon TCR signaling is independent of canonical Hh signaling via Ihh and Smo

Given the role of Smo in maintaining Gli1 steady-state protein expression [10] we asked
275 whether canonical Hh signaling was needed for the induction of Gli1 after TCR stimulation. To investigate this, we generated two different conditional knockout lines (Suppl. Fig. 5A,B). For the first mouse line, we crossed *GzmB ER^{T2}Cre* mice [26] to *Smo^{f/f}* mice, to generate mice in which Cre is only active in mature CTLs. The second mouse line was generated by crossing *dLckCre* mice to *Ihh^{f/f}* mice, in which the Cre is active only
280 after T cell development has been completed in the thymus. Ihh is the only Hh ligand expressed by $CD8^+$ T cells and Hh signaling has been suggested to be entirely intracellular in $CD8^+$ T cells [10]. We therefore decided to knock out endogenous Ihh in $CD8^+$ T cells as well as Smo the key signal transducer of canonical Hh signaling. Importantly, the peripheral T cell compartment in conditional *Ihh* KO mice and inducible
285 *Smo* KO mice is normal (Suppl. Fig. 5A,B). Interestingly, $CD8^+$ T cells from *Smo^{f/f}* and *Ihh^{f/f}* mice showed a modest reduction of *Gli1* mRNA at steady state but upregulated *Gli1* mRNA to the same extent as WT cells upon TCR stimulation (Fig. 5B,C), indicating that Gli1 induction upon TCR signaling is not mediated by canonical Hh signaling.

Ca^{2+} is required for the binding of Ihh to Ptch [22], thought to initiate canonical Hh signaling
290 in $CD8^+$ T cells. To confirm that canonical Hh signaling is indeed independent of our newly identified Ca_v1-regulated Gli1 induction, we treated CTLs from *Ihh^{+/fl}* and *Ihh^{fl/fl}* mice with Nifedipine and U0126. We observed the same levels of inhibition of Gli1 induction in both conditions (Fig. 5C), suggesting that the MAPK-Ca_v-Gli1 axis is independent of canonical Hh signaling.

295 We also considered whether overexpression of either Ihh or Smo would further increase Gli1 induction. For this we transduced primary $CD8^+$ T cells with retroviruses encoding Ihh or a constitutively active form of Smo (SmoM2) [27], resulting in 80000- and 300-fold overexpression, respectively (Suppl. Fig. 5C). Strikingly, we did not observe any further

10

300   increase in the induction of Gli1 as compared to empty vector-transduced control CD8$^+$ T cells. (Fig. 5D).

Thus, canonical Hh signaling via Ihh and Smo is not responsible for the induction of Gli1 downstream of the TCR, and is independent of the MAPK and L-type voltage-gated Ca^{2+} channel-induced Gli1 activation.

305

DISCUSSION

In this manuscript we have uncovered a novel non-canonical Hh signaling pathway
310   whereby a Ca$_v$1 channel-mediated Ca^{2+} flux can induce Gli1. We show that this mechanism of Gli1 induction is functionally critical for CTL killing, providing a direct mechanistic link between Ca$_v$1 channels and CTL killing (Fig. 5E).

There is currently great scientific interest to unmask the roles of Ca$_v$ channels in T cell
315   biology. Constitutive knockout of Ca$_v$1.4 or the Ca$_v$ channel regulatory β3 subunit leads to signaling defects in thymocytes and apoptosis of peripheral T cells, respectively [13]. This makes it challenging to draw conclusions about the role of Ca$_v$ channels in mature peripheral T cells. Here we use CRISPR technology to functionally ablate Ca$_v$ channels in primary mature T cells only.
320   All four family members of the L-type Ca^{2+} channels (Ca$_v$1.1, Ca$_v$1.2, Ca$_v$1.3, and Ca$_v$1.4) are expressed in murine T cells [24] and we find that only Ca$_v$1.4 and to a lesser extent Ca$_v$1.3 are expressed in human CD8$^+$ T cells. We show that Ca$_v$1.3 and Ca$_v$1.4 (and to a lesser extent Ca$_v$1.1) are involved in the induction of Gli1 in CD8$^+$ T cells. Apart from the localization of Ca$_v$1.4 to lipid rafts little is known about the cellular localization of Ca$_v$
325   channels [12]. Here we find that Ca$_v$1.4 is expressed at the plasma membrane and on intracellular vesicles in primary human CD8$^+$ T cells.

There is evidence from the literature that in neuronal cells canonical Hh signaling can induce Ca^{2+} spikes via Ca$_v$ and TRPC1 channels [7]. Here we show that the "reverse" is

11

330 true in T cells, where we show that Ca^{2+} signaling via Ca_v channels induces Hh signaling. Our work uncovers Ca^{2+} signaling via Ca_v channels as a novel mechanism of non-canonical, Ptch/Smo-independent Hh signaling.

 The literature supports the notion that our proposed Ca_v-Gli axis may be active in other cells. Humans with mutations in Ca_v channels phenotypically display heart arrhythmias

335 and signs of autistic spectrum disorder (consistent with the critical roles of Ca_v channels in the heart and brain) as well as signs of syndactyly [28], a phenotype which has been robustly linked to inactivating mutations in the Hh pathway [29]. Furthermore, studies in mice showed that knockdown of Ca_v channels leads to abnormalities in skeletal development [30], highly reminiscent of the defects observed in *Ihh* KO mice [31]. These

340 studies suggest that loss-of-function phenotypes of Ca_v channels phenotypically mimic known Hh loss-of-function phenotypes, consistent with the hypothesis that a Ca_v-induced mechanism of Gli activation is operational in other cell types.

 Interestingly, we uncover that in CTLs MAPK activation downstream of the TCR critically

345 contributes to Gli1 transcription which has been shown in other cell types and cancers [11]. Of interest is the difference of Gli1 regulation between naïve CD8+ T cells, that seem to solely rely on Ca_v signaling, and CTLs, that also employ MAPK signaling. A possible explanation for this could be that naïve CD8+ T cells have much longer contact times with an APC and form more stable synapses *in vivo* when they are stimulated than CTLs,

350 which have shorter contact times with their target cells and have been shown to often require multiple rounds of contact *in vivo* to efficiently kill target cells [32]. Therefore, CTLs may have evolved two pathways to ensure appropriate levels of Gli1 activation.

 We show that Gli1 activation by Ca_v channels is important for killing in murine and human

355 CD8+ T cells (Fig. 5A, Fig. 4E) which is a rapidly-induced process with killing observed within a few hours *in vitro*. This is consistent with findings in the literature that Gli1 activation can be rapidly induced [33], but the question remains how the transcription factor Gli1 can exert its effect on killing in such a short timeframe. Given that Gli1 can regulate the cytoskeleton [10], we hypothesize that Gli1-induced transcription in CTLs upon target

360   recognition is required for cytoskeletal rearrangement and immune synapse formation upon successive target cell contacts and serial killing.

Regarding the activation of Ca_v channels in T cells, it is tempting to speculate that this is PKC-driven because of two observations. First, Ca_v channels in T cells lack the ability to respond to depolarization and instead become activated upon TCR engagement [34]. And

365   second, PKC is a well-known activator of Ca_v channels in excitable cell types and has been hypothesized as the link between TCR and Ca_v channel activation in T cells [35, 36]. This would explain why we find that PMA (a PKC agonist) is able to drive Gli1 induction (Fig. 2B), particularly in naïve CD8^{+} T cells where this effect cannot simply be explained by PKC-related induction of MAPK signaling (which has no effect on Gli1 induction). The

370   requirement for PKC for Ca_v activation and the different nature of the Ca^{2+} flux induced by ionomycin might also explain why ionomycin administration alone cannot induce Gli1.

The precise mechanism by which Ca_v1 channel activation results in Gli1 induction is not known at this point. One potential mechanism is via Ulk family proteins that can be

375   activated by Ca^{2+} and have been shown to activate Gli1 via proteolytic cleavage in a very short timeframe [33, 37]. And indeed we find Ulk3 expressed in CD8^{+} T cells (Suppl. Fig. 5D).

Canonical Hh signaling is active for long periods of time, is initiated by extracellular

380   ligands, and computes a cell fate choice [3]. By contrast, CTL killing must happen much more rapidly and should not rely on extracellular ligand gradients. Canonical Hh signaling is a more ancient signaling pathway than TCR signaling [2]. The pathway might have come under evolutionary pressure for the induction of Gli1 to be more rapid and isolated from extracellular signals resulting in direct activation by the TCR.

385

Taken together, we show that Gli1 is critical for CD8^{+} T cell killing of tumor cells and that Gli1 activation is intricately coupled to CD8^{+} T cell activation downstream of the TCR via Ca_v channels. Our findings have clinical implications. Gli inhibitor Arsenic Trioxide (ATO) is currently in clinical trials for the treatment of various cancers including advanced Basal

390   Cell Carcinoma and Acute Myeloid Leukemia [38]. Our data suggests that ATO may inhibit

13

the CD8$^+$ anti-tumor response and might explain why Gli1 inhibitors have had little success in the clinic so far.

395

MATERIALS AND METHODS

Mice

RAG2KO were a generous gift from Suzanne Turner (University of Cambridge) and OTI mice were purchased from the Jackson Laboratory (C57BL/6-Tg(TcraTcrb)1100Mjb/j, Stock

400 no. 003831). OTI RAG2KO mice were generated from these. *Gli1-eGFP* mice were a generous gift from Alexandra Joyner (Sloan Kettering Institute)[39] and were backcrossed onto the C57BL/6J background (The Jackson Laboratory, Bar Harbor, ME) for more than 11 generations. *dLckCre* and *ROSA26tdTom* mice were a generous gift from Randall Johnson and Douglas Winton (University of Cambridge), respectively. GzmBER^{T2}*Cre/ROSA26EYFP*

405 mice were a generous gift from D. T. Fearon (Cold Spring Harbor Laboratory)[26] and were backcrossed onto the C57BL/6J background (The Jackson Laboratory, Bar Harbor, ME) for more than 11 generations. *Smo$^{f/f}$* (Smo^{tm2Amc}/J, Stock no. 004526*)* and *Ihh$^{f/+}$* (*Ihh^{tm1Blan}*/J**, Stock no. 024327) mice were purchased from The Jackson Laboratory. *Smo$^{fl/fl}$* mice were back-crossed to the C57BL/6J background (Charles Rivers Inc., UK) for more than 10

410 generations and crossed to GzmBER^{T2}*Cre/ROSA26EYFP* mice to generate *GzmBER^{T2}Cre/ROSAEYFP/Smo$^{fl/fl}$* mice. *Ihh$^{fl/fl}$* mice were crossed onto *dLckCre/ROSA26tdTom* mice.

Mice were maintained at the CRUK Cambridge Institute/ University of Cambridge, genotyped using Transnetyx, and used at 6-8 weeks of age. All housing and procedures

415 were performed in strict accordance with the United Kingdom Home Office Regulations.

Cell Culture

14

420 Purified naïve murine CD8$^+$ T cells were cultured at 1x10^6 cells/ml in complete RPMI media: RPMI (Gibco, Cat no. 21875034) supplemented with 5% heat-inactivated batch-tested FCS (Biosera, Cat no. 1001-500ml), 50µM β-Mercaptoethanol (50mM, Gibco, Cat no. 31350-010), 100U/ml Penicillin/Streptomycin (10'000 U/ml, Gibco, Cat no.15140-122), 1µM Sodium Pyruvate (Gibco, Cat no. 11360039), 10µM HEPES (Sigma, Cat no. H0887) and 10ng/ml murine IL-2 (Peprotech, Cat no. 212-12). Human CD8$^+$ T cells were cultured in ImmunoCult cell culture media (Stemcell Technologies, Cat no. 10981) supplemented with 425 35 ng/ml human IL-2 (Peprotech, Cat no. 200-02).

HEK 293T cells and P815 cells were cultured in DMEM (Gibco, Cat no. 21885-025) supplemented with 10% heat-inactivated FCS (Biosera, Cat no. 1001-500ml). EL-4 cells were cultured in RPMI supplemented with 10% heat-inactivated FCS.

All cells were grown in a humidified incubator at 37ºC and 5% CO_2 and cell lines tested 430 mycoplasma negative (MycoProbe® Mycoplasma Detection Kit, R&D systems).

CD8$^+$ T cell isolation and activation

Mouse

Spleens were harvested and cell suspensions made. Naïve murine CD8$^+$ T cells were 435 isolated using negative selection (Naïve CD8 T Cell Isolation Kit, Cat no. 130-096-543, Miltenyi Biotec) according to the manufacturer's instructions. The purity of the sorted populations was above 95%. CD8$^+$ T cells were stimulated with platebound anti-CD3ε (1µg/ml, eBioscience, Cat no. 16-0033-86) and anti-CD28 (2µg/ml, eBioscience, Cat no. 16-0281-86) antibody.

440 For CTL generation, a splenocyte suspension from one OT-I Rag2$^{-/-}$ spleen was stimulated with 10nM Ova$_{257-264}$ peptide (SIINFEKL, AnaSpec, Cat no. 60193-5-ANA) for 48h and cultured for up to 10 days. Cells were restimulated with plate-bound anti-CD3ε (2.5µg/ml).

Human

15

445   Buffy Coats from healthy donors were acquired from NHS Blood and Transplant (Cambridge) under appropriate ethics (Research into Altered Lymphocyte Function in Health and Disease, REC reference: 17/YH/0304). PBMCs were isolated using SepMate PBMC Isolation Tubes (Stemcell Technologies, Cat no. 86450) according to the manufacturer's instructions and naïve CD8$^+$ cells were obtained using the MojoSort Human CD8$^+$ Naïve T Cell Isolation Kit (Biolegend, Cat no.480045). Purity was consistently over >75% CD8$^+$ with

450   no contamination of CD4+ T cells and >80% of CD8+ T cells being naive. Cells were >95% CD8$^+$ on day 1of stimulation. Naïve CD8$^+$ cells were plated with Human T-Activator CD3/CD28 Dynabeads (Thermofisher, Cat no.111.31D) at 25 µl of Dynabeads per 1x10^6 CD8$^+$ cells in complete ImmunoCult cell culture media (see above). On day 3, the beads were magnetically removed. When indicated, the cells were re-stimulated on d10 with 12.5

455   µl of Dynabeads per 1x10^6 CD8$^+$ cells for three additional days. On d14, the beads were removed.

CRISPR knockout of primary CD8$^+$ T cells

    Ribonucleoprotein (RNP) complexes were assembled following the manufacturer's

460   instructions using Alt-R$^®$ CRISPR-Cas9 crRNA (IDT) and tracrRNA (IDT, Cat no. 1072534). CD8$^+$ T cells were isolated from OT-I Rag2$^{-/-}$ spleens and stimulated with plate-bound anti-CD3ε/CD28 antibodies in complete RPMI media. After 48h of stimulation, cells were washed twice in pre-warmed PBS (Gibco) prior to resuspension in 80µl Buffer T (10^6 cells/electroporation reaction). The suspension was briefly mixed with the RNP complex

465   solution prior to electroporation with the Neon™ electroporation system in 100µl electroporation tips (Thermo, Cat no. MPK10096) with three pulses of 1600V each with a pulse width of 10ms. Cells were left to recover in complete RPMI in the absence of antibiotics for 20min. Cells were then centrifuged at 1500rpm for 5min and returned into culture in complete RPMI media (without antibiotics). Antibiotics were re-added after six hours at the

470   indicated concentration.

Guide	Sequence (5'→ 3')
Non-targeting control 1	Proprietary (IDT, Cat No. 1072544)

16

Non-targeting control 1	Proprietary (IDT, Cat No. 10725455)
Ca$_v$1.1#1 (CACNA1S)	AGCAAGAUGAUGGUCUCGAA
Ca$_v$1.1#2 (CACNA1S)	TGAAGAGGGTCAGCAACACG
Ca$_v$1.2#1 (CACNA1C)	CTACCGTCAGTTCCACACAG
Ca$_v$1.2#2 (CACNA1C)	CTACCGTCAGTTCCACACAG
Ca$_v$1.3#1 (CACNA1D)	GTCGAAGTGGTCTTAACACT
Ca$_v$1.3#2 (CACNA1D)	TCTGAACATGGTCTTCACAG
Ca$_v$1.4#1 (CACNA1F)	GTTCCTGGTGATTTTCACCG
Ca$_v$1.4#2 (CACNA1F)	TCCTGAGGAGACGTACACAT

Table 1. List of crRNA used for CRISPR in CD8$^+$ T cells

Genome editing efficiency assay

Genomic DNA was extracted from T cells using a DNeasy Blood & Tissue kit (Qiagen, Cat no. 69506). PCR amplification of the region of gDNA containing the CRISPR editing locus was performed using the SequalPrep Long PCR Kit with dNTPs (Invitrogen, Cat no. A10498) according to the manufacturer's instructions. Primers (Sigma) used were as follows:

Primer	Sequence (5'→3')
Cacna1d forward	TGGACACTTTGTTGGCATGA
Cacna1d reverse	AGTTTTACCAAGGGCAGAGC
Cacna1f forward	CCACAACTTGGTGAGGTCTA
Cacna1f reverse	GAGGTCGTAGCACCCTAAAT

Table 2: PCR Primers used for genome editing efficiency assays

A T7 endonuclease I mismatch cleavage assay was performed using the Alt-R® Genome Editing Detection Kit (IDT, Cat no. 1075932) per the manufacturer's instructions.

17

Quantification of cleaved bands was performed on a capillary electrophoresis system (4200 Tapestation, Agilent) using D5000 screentape (Agilent, Cat no. 5067-5588/9).

485 ### *In vitro* killing assay

CD8$^+$ T cell cytotoxicity was assessed using a Cyto Tox 96® Non-radioactive Cytotoxicity Assay kit (Promega, Cat no. G1780) according to the manufacturer's instructions. Murine and human CTLs were generated as previously described and used on day 6/7 or day 14/15 post-stimulation, respectively. EL-4 cells were used as target cells for murine OTI CTLs and

490 pulsed for 1h at 37°C with 1μM SIINFEKL. P815 cells were used as target cells for human CTLs and pulsed for 1h at 37°C with 1μg/ml anti-CD3 antibody (clone UCHT1, Biolegend, Cat no. 300438). They were washed and resuspended at 1x10^5 cells/ml in killing assay media (RPMI without phenol red + 2% FCS) in a round-bottom 96 well plate.

T cells were washed, resuspended in killing assay media and plated at the indicated

495 effector:target ratios. Plates were incubated at 37°C prior to collection of supernatant at the designated timepoints. Absorbance was measured at 490nm using a CLARIOstar microplate reader (BMG Labtech).

Flow cytometry and FACS

500 *Surface staining*

Cells were stained with fixable viability dye eFluor780 (eBioscience, Cat no. 65-0865-18) or DAPI (Thermo Fisher, Cat no. D9542, 1:3000 in PBS), washed, and incubated with Fc block (1:100; Biolegend TruStain fcX, cat no. 101320) and fluorophore-conjugated antibodies at the appropriate concentrations (Table 3) for 20min at 4°C.

505 *Intracellular staining*

Following surface staining, cells were fixed with BD Cytofix/Cytoperm Plus Fixation Buffer (BD Biosciences, Cat no. 554715) as per manufacturer's instructions and stained with fluorophore-conjugated antibodies at the appropriate concentrations (Table 3) for 30min at

18

4°C. Prior to analysis, cells were washed once in permeabilization buffer and once in FACS
510   buffer.

pErk staining

Naïve CD8^{+} T cells or CTLs were isolated/maintained as described previously. Cells were
pre-incubated for 30min at 37°C with 10μM MEK1/2 inhibitor U0126 (Cambridge
Biosciences, Cat no. SM106-5) or carrier control (DMSO). Cells were stimulated by
515   crosslinking the TCR using 10μg/ml soluble anti-CD3ε and 5μg/ml soluble anti-CD28 with
the addition of goat-anti-hamster IgG (1:300) for 2min in a 37°C waterbath. Cells were fixed
in 2% PFA (EMS, Cat no. 15710-S), washed and incubated in BD Phosflow Lyse/Fix Buffer
(BD, Cat no. 558049) for 10min at 37°C. Cells were washed with BD Phosflow Perm/Wash
I Buffer (BD, Cat no. 557885) and stained with primary anti-pErk antibody(30min, 4°C) and
520   then secondary anti-Rabbit Alexa Fluor 647 and anti-CD8a PE antibodies at the indicated
concentrations (Table 3) (20min, 4°C).

Flow cytometric analyses were conducted on a BD LSRII or BD LSR Fortessa cell analyser,
and data was analysed with FlowJo software (Tree Star Inc., version 10.4).

Target	Clone	Reactivity	Fluorochrome	Dilution	Cat no.	Supplier
CCR7	G043H7	Human	PE/Cy7	1:50	353226	Biolegend
CD3ε	145-2C11	Mouse	BUV395	1:50	583565	BD
CD3ε	UCHT1	Human	BUV395	1:100	563556	BD
CD4	RM4-5	Mouse	BV605	1:200	100548	Biolegend
CD4	RM4-5	Mouse	APC	1:200	100516	Biolegend
CD4	RM4-5	Mouse	FITC	1:200	100510	Biolegend
CD4	RM4-5	Mouse	PE	1:200	100512	Biolegend
CD4	RPA-T4	Human	BV605	1:100	300556	Biolegend
CD8a	53-6.7	Mouse	BV605	1:200	100744	Biolegend
CD8a	53-6.7	Mouse	APC	1:200	100712	Biolegend
CD8a	53-6.7	Mouse	FITC	1:200	100706	Biolegend
CD8a	53-6.7	Mouse	PE	1:200	100707	Biolegend

19

CD8	RPA-T8	Human	BV711	1:100	301044	Biolegend
CD27	LG.3A10	Human	PerCP/Cy5.5	1:50	124214	Biolegend
CD28	CD28.2	Human	BV785	1:50	302950	Biolegend
CD44	IM7	Mouse/Human	BV785	1:400	103059	Biolegend
CD44	IM7	Mouse/Human	BV711	1:400	103057	Biolegend
CD44	IM7	Mouse/Human	PE/Cy7	1:400	103030	Biolegend
CD45	30-F11	Mouse	PE/Cy7	1:200	103114	Biolegend
CD45	HI30	Human	FITC	1:100	304006	Biolegend
CD45RO	UCHL-1	Human	APC	1:100	304210	Biolegend
CD62L	MEL-14	Mouse	BV421	1:200	104436	Biolegend
CD62L	MEL-14	Mouse	BV510	1:200	104441	Biolegend
CD90.1	HIS51	Mouse/Rat	APC	1:200	17-0900-82	BD
CD90.1	HIS51	Mouse/Rat	PE	1:200	12-0900-83	Thermo
CD95	DX2	Human	BV421	1:50	305624	Biolegend
IFNγ	XMG1.2	Mouse	BV711	1:100	505835	Biolegend
IL-2	JES6-5H4	Mouse	PE	1:100	503808	Biolegend
TCRβ	H57-597	Mouse	BV711	1:200	109243	Biolegend
TCR$\gamma\delta$	GL3	Mouse	Alexa Fluor 488	1:200	118128	Biolegend
pErk	197G2	Mouse/Human	none	1:200	4377	Cell Signaling
p65	532301	Mouse/Human	APC	1:20	IC5078A	R&D Systems
Rabbit IgG	Polyclonal	Rabbit	Alexa Fluor 647	1:500	A-21245	Thermo Fisher

525

Table 3: List of antibodies used for flow cytometry

In vitro tamoxifen treatment

In vitro tamoxifen was given as 4-hydroxytamoxifen (4-OH-Tamoxifen or OHT) (TOCRIS, Cat no. 3412) solubilized in DMSO (Life Technologies, Cat no. D12345) in order to activate CreER^{T2} recombinase _in vitro_. Stock solutions were made at 100mM and kept at -20ºC

530 protected from light. Cells were treated at a concentration of 300nM, diluted in complete

20

RPMI (Gibco), and fresh 4-OHT was added daily for the duration of culture. Control-treated cells received DMSO in complete RPMI.

Small molecule treatment of CD8^{+} T cells

For small molecule treatment studies, naïve CD8^{+} T cells or CTLs were incubated for 1h (2h in the case of BTP2 –[40]) prior to (re-)stimulation. Doses of Ca^{2+} channel blockers were chosen based on doses established for use in T cells in the literature (see Table 4). All inhibitors were reconstituted in DMSO (Life Technologies, Cat no. D12345) according to the manufacturer's instructions and a carrier control was included for all experiments. The small molecules used were as follows:

Inhibitor	Dose(s)	Stock concentration	Manufacturer	Cat no.
PMA	1, 5, 10, 50ng/ml	1mg/ml	Sigma	P1585
Ionomycin	10, 50, 100, 1000ng/ml	1mg/ml	Sigma	I9657
U0126[18]	10µM	Reconstituted freshly	Cambridge Bioscience	SM106-5
BAPTA-AM[41]	1.25, 2.5, 5, 10, 25µM	Reconstituted freshly	Thermo Fisher	B1205
TNP-ATP[42]	30µM	10mM	Tocris	2464/5
BCTC[43]	1µM	10mM	Tocris	3875/10
BTP2 (YM-58483)[40]	200nM	5mM	Tocris	3939/10
HC030031[44]	100µM	100mM	Tocris	2896/10
Nifedipine[45]	10, 50, 100µM	100mM	Tocris	1075/100

Table 4: Overview of small molecules used

qRT-PCR

Cells harvested for RNA extraction were washed twice in ice-cold PBS, snap-frozen as dry pellets, and stored at -80°C. RNA was extracted using the RNAqeous™-Micro Total RNA

Isolation Kit (murine cells) or the Single Cell RNA Purification Kit (Norgen Biotek Corp., cat no. 51800) (human cells) according to the manufacturer's instructions. RNA concentration was measured with a Nanodrop spectrophotometer (Labtech ND-1000) and samples were stored at -80°C if not used immediately.

550 Reactions for qRT-PCR were set up using the One-Step qRT-PCR Kit (Thermo Fisher SuperScript III Platinum, cat no. 11732088) according to the manufacturer's instructions.

Probe	Cat no.	Exon Boundary
CD3ε	Mm00599684_g1	6-7
Tbp	Mm00446973_m1	4-5
Tbp	Mm00446971_m1	2-3
Ihh	Mm01259021_m1	1-2
Smo	Mm01162710_m1	8-9
Gli1	Mm00494654_m1	11-12
Gli1	Mm00494645_m1	2-3
Ulk3	Mm01151463_m1	4-5
CACNA1F	Hs00913730_m1	46-47
CACNA1D	Hs00167753_m1	46-47
CACNA1S	Hs00163885_m1	2-3
CACNA1C	Hs00167681_m1	3-4
TBP	Hs00427620_m1	2-3
GLI1	Hs01110766_m1	8-9

Table 5: Taqman probes (Thermo Fisher) used for qRT-PCR

555 Each sample was run in triplicate with *Tbp* and/or *CD3ε* used as housekeeping genes. In addition, each experiment included a non-template control and primer/probes were validated by no RT controls. Samples were run on a QuantStudio 6 Flex Real-Time PCR System

22

(Thermo Fisher). Levels of Gli1 mRNA were determined using probe (Mm00494654_m1) and confirmed in some of the experiments with a second probe (Mm00494645_m1).

560 Expression of the gene transcript of interest was calculated with the ΔCt method [46]. The cycle threshold (Ct) value from the gene of interest was subtracted from the housekeeping gene and transformed with a factor of 2^(-ΔCt) to give the fold expression relative to the housekeeping gene.

565 **Immunofluorescence**

Primary human CTLs at day 11 post-stimulation were plated onto glass slides at 4×10^6/ml and allowed to adhere to the glass for 10min at 37°C in an incubator. Cells were fixed with 4% PFA (16% PFA solution, CN Technical Services, cat no. 15710-s, 1x PBS) for 10min at room temperature. Slides were washed 5 times with PBS and blocked with

570 blocking buffer (PBS + 1% bovine serum albumin (BSA, Sigma, cat no. A3912; 50 g lyophilized powder) + 0.1% TritonX-100 (Alfa Aesar)) for 30min at room temperature. Blocking buffer was aspirated and blocking buffer containing primary rabbit anti-Cav1.4 (1:50, Stratech, Cat no. LS-C94032-LSP) antibody was added. After staining for one hour at room temperature slides were washed 5 times with PBS + 0.1% TritonX-100. Anti-

575 rabbit AlexaFlour 488 secondary antibody (1:400 dilution, Thermo, Cat No. A11034) as well as phalloidin (1:100, Thermofisher, Cat no. A12380) were added in blocking buffer (PBS + 1% BSA + 0.1% TritonX-100) and slides were incubated for 30min light-protected at room temperature. After incubation, slides were washed 5 times with PBS + 0.1% TritonX-100 and stained with Hoechst (Hoechst 33342, trihydrochloride, trihydrate

580 Invitrogen/Fisher, cat no. H3570, 1:30,000 dilution) prepared in PBS for 5min light-protected at room temperature. Slides were washed five times with PBS and mounted with ProLong Diamond Antifade Mountant (Fisher, cat no. P36961).

For conjugate staining, primary human CTLs at day 14/15 post-stimulation (on d0 and d10) were conjugated for 30min at 37°C with P815 target cells at a 1:1 ratio. P815s were

585 pre-stained with 25µM CellTracker Red CMTPX Dye (Thermofisher, Cat no. C34552) for 45min at 37°C and simultaneously pulsed with 1µg/ml CD3 (UCHT1). The staining was

23

comprized of rabbit anti-Cav1.4, phalloidin (1:100, Thermofisher, Cat no. A22287), donkey anti-rabbit 488 and Hoechst 33342, as above.

Confocal spinning disc microscopy was performed on an Andor Dragonfly 500 (Oxford Instruments) and images were processed using Imaris software (Bitplane/Oxford Instruments).

Western Blot

Cells were lysed in ice-cold RIPA buffer (150mM NaCl, 50mM Tris-HCl pH 8.0, 1mM MgCl$_2$, 2% Triton) with protease inhibitor (Pierce, Cat. No. 88666). Samples were heated at 65°C for 15min and loaded together with a protein standard (Bio Rad, Cat no. 161-0394), onto a NuPAGE 4-12% gradient Bis/Tris Acrylamide gel (Thermo Fisher, Cat no NP0335BOX). PAGE was run in Nu-PAGE MOPS running buffer (Thermo Fisher, Cat no. NP0001). Western Blotting was performed using wet transfer in Nu-PAGE Transfer Buffer (Thermo Fisher, Cat no. NP0006-01) + 10% Methanol (Honeywell, Cat no. 32213-2.5L). Membranes were blocked with 5% (w/v) nonfat dry milk (Marvel Original, Dried Skimmed Milk) in TBS before incubation with primary and secondary antibodies. Membranes were developed with SuperSignal West Pico Plus Chemiluminescent Substrate (Thermo Fisher, Cat no. 34580).

Target	Clone	Reactivity	Type	Dilution	Cat no.	Supplier
Gli1	388516	Mouse/Human	Primary	1:1'000	MAB3324	Biotechne
β-tubulin	Polyclonal	Rabbit anti-human/rat/mouse	Primary	1:2'000	2146	Cell Signaling
Rat IgG	Polyclonal	Goat anti-rat	Secondary (HRP conj.)	1:3'000	7077S	Cell Signaling
Rabbit IgG	Polyclonal	Donkey anti-rabbit	Secondary (HRP conj.)	1:10'000	P0448	Dako

Table 6: Antibodies used for Western Blotting

Retroviral transduction

Generation of retrovirus

610 One day prior to the generation of retrovirus, HEK 293T cells were seeded in a six well plate resulting in 75% confluency the next day. Media was replaced with 2ml fresh DMEM per well prior to transfection with retroviral plasmids. HEK 293T cells were transfected with 1.5µg of packaging plasmid pCL-Eco (generous gift from Gillian Griffiths, Cambridge UK) and 1.9µg pMig vector – either 5'LTR-eGFP-IRES-rThy1.1(CD90.1)-3'LTR (referred

615 to as "empty vector"), 5'LTR-Smo-C terminal eGFP fusion-STOP-IRES-rThy1.1(CD90.1)-3'LTR (referred to as "SmoM2") or 5'LTR-Ihh-STOP-IRES-rThy1.1(CD90.1)-3'LTR (referred to as "Ihh") – prepared in Opti-MEM™ media (Gibco, Cat no. 31985070). Concurrently, a 1:25 dilution of Lipofectamine™ 2000 (Invitrogen, Cat no. 11668019) was prepared in Opti-MEM™ media. The DNA-Opti-MEM™ solution was mixed with the

620 Lipofectamine™2000-Opti-MEM™ solution at a ratio of 1:1 and incubated for 5min at room temperature after which 400µl of the mixture was added drop-wise to the HEK-293T cells. Media was replaced 18h after transfection and collected 48h post transfection. The retroviral supernatant was passed through a 0.45µm PVDF membrane filter (Merck Millipore, Cat no. SLHVM33RS) for immediate use.

625 *Retroviral transduction of CD8$^+$ T cells*

Naïve CD8$^+$ T cells were isolated from C57BL/6 spleens and stimulated with plate bound anti-CD3ε/CD28 antibodies as described previously. After 24h of stimulation, T cell media was partially withdrawn and replaced by retroviral supernatant in a 1:2 ratio supplemented with protamine sulphate (Sigma, Cat no. 1101230005) at a final concentration of 9µg/ml

630 and IL-2 to maintain the standard CD8$^+$ T cell polarization conditions as described above. Cells were then centrifuged at 1800rpm for 15min at 32°C and subsequently placed in a humidified cell culture incubator. 48h cells were centrifuged to wash off retroviral supernatant and cultured after that in complete RPMI + IL-2.

Magnetic sorting of retrovirally transduced cells

25

635 For downstream applications such as qRT-PCR, retrovirally transduced cell populations were enriched for transduced cells measured by the presence Thy1.1 expression. T cell populations were subjected to magnetic sorting at day 3 or 4 after initial stimulation. Thy1.1$^+$ cells were positively enriched using the EasySep™ PE Positive Selection Kit (Stem Cell Technologies, Cat no. 17684) or EasySep™ Release Mouse PE Positive

640 Selection Kit (Stem Cell Technologies, Cat no. 17656) according to the manufacturer's instructions. Cells were labelled with a PE-conjugated Thy1.1 antibody (Clone HIS51, BD, Cat No. 12-0900-81) at a final concentration of 0.25mg/ml in MACS buffer. All steps were performed in MACS buffer and all incubations were performed at room temperature. PE positive cells were enriched using an EasyEights™ magnet (Stem Cell Technologies, Cat

645 no. 18103). Three rounds of separation were performed in total and cells were washed in complete media prior to maintenance in culture with complete RPMI + IL-2. Purity of the sort was routinely over 95% as measured by FACS.

Nucleofection of CTLs

650 The GFP-VIVIT plasmid was a gift from Anjana Rao (Addgene Plasmid # 11106; http://n2t.net/addgene:11106; RRID:Addgene_1106) which contains a fusion of MAGPHPVIVITGPHEE to the N-terminus EGFP, resulting in selective inhibition of the interaction between calcineurin and NFAT[16]. The IκBα dominant negative ("IκB DN") plasmid was a generous gift from Felix Randow (Laboratory of Molecular Biology,

655 Cambridge). The plasmid contains an IκBα which is resistant to proteosomal degradation due to two amino acid substitutions (S32→A32 and S36→A36) resulting in a dominant-negative phenotyping inhibiting NF-κB induced transcription[17].

Splenocytes from one OT-I Rag2$^{-/-}$ mouse were stimulated with 10nM Ova (SIINFEKL) peptide for 48h and subsequently washed daily (resuspended at 1x10^6 cells/ml). On day

660 6 CTLs were subjected to lympholyte treatment (Cedarlane, CL5035) per the manufacturer's instructions. On day 7 cells were nucleofected using the Amaxa Mouse T Cell Nucleofector Kit (Lonza, Cat no. VVPA-1006) per the manufacturer's instructions with 5x10^6 cells and 1.5µg plasmid DNA per cuvette. Cells were electroporated using a

665   Nucleofector 2b Device (Lonza) on programme X-001. Cells were restimulated 18h post nucleofection on day 8.

ImageStream analysis of NF-κB nuclear translocation

On day 8, 18h after nucleofection, CTLs were counted and plated onto a 24-well plate pre-coated overnight with 2.5μg/ml anti-CD3ε antibody. After 1h of stimulation, cells were
670   harvested and washed once in PBS prior to staining with eFluor780 for 10min light-protected at room temperature. Cells were subsequently washed in perm wash buffer – made up of 2% FCS, 0.1% Sodium Azide, 0.1% Triton X-100 (Alfa Aesar, Cat no. A16046.AE) in PBS prior to fixation in 4% PFA for 10min light-protected at room temperature. Cells were washed twice in perm wash buffer before staining in 100μl perm
675   wash buffer containing anti-p65 APC antibody (Table 4) for 30min light-protected at room temperature. Cells were washed twice in perm wash buffer, subsequently resuspended in 50μl perm wash buffer and transferred to a 1.5ml Eppendorf tube. DAPI was added (0.5mg/ml) immediately prior to acquisition on an Amnis ImageStream (MilliporeSigma) imaging cytometer. Data was analysed with IDEAS Software (MilliporeSigma).

680

Analysis of Chip-Seq data

Coverage bigwig files were downloaded from GEO (GSE54191). The Integrative Genomics Viewer (IGV) was used for coverage analysis[47].

685

DATA AVAILABILITY

This study includes no data deposited in external repositories.

690

ACKNOWLEDGEMENTS

FUNDING

710   **AUTHOR CONTRIBUTION**

MdlR and JH conceived the project and designed the experiments. JH executed most experiments. CK performed experiments with human CD8$^+$ T cells with assistance from FB. LMOB and VC performed experiments and helped with technical expertise, and Chandra Chilamakuri analysed Chip-Seq data. JH and MdlR analyzed the results and
715   wrote the manuscript.

CONFLICTS OF INTEREST

The authors declare that they have no conflict of interest.

720

REFERENCES

1.   de la Roche, M., Asano, Y. & Griffiths, G.M. Origins of the cytolytic synapse. *Nat Rev Immunol* **16**, 421-432 (2016).

2.   Griffiths, G.M., Tsun, A. & Stinchcombe, J.C. The immunological synapse: a focal point for endocytosis and exocytosis. *J Cell Biol* **189**, 399-406 (2010).

3.   Briscoe, J. & Therond, P.P. The mechanisms of Hedgehog signalling and its roles in development and disease. *Nat Rev Mol Cell Biol* **14**, 416-429 (2013).

4.   Chen, X.L. *et al.* Patched-1 proapoptotic activity is downregulated by modification of K1413 by the E3 ubiquitin-protein ligase Itchy homolog. *Mol Cell Biol* **34**, 3855-3866 (2014).

5.   Polizio, A.H., Chinchilla, P., Chen, X., Manning, D.R. & Riobo, N.A. Sonic Hedgehog activates the GTPases Rac1 and RhoA in a Gli-independent manner through coupling of smoothened to Gi proteins. *Sci Signal* **4**, pt7 (2011).

6.   Sasaki, N., Kurisu, J. & Kengaku, M. Sonic hedgehog signaling regulates actin cytoskeleton via Tiam1-Rac1 cascade during spine formation. *Mol Cell Neurosci* **45**, 335-344 (2010).

7.   Belgacem, Y.H. & Borodinsky, L.N. Sonic hedgehog signaling is decoded by calcium spike activity in the developing spinal cord. *Proc Natl Acad Sci U S A* **108**, 4482-4487 (2011).

8.   Pietrobono, S., Gagliardi, S. & Stecca, B. Non-canonical Hedgehog Signaling Pathway in Cancer: Activation of GLI Transcription Factors Beyond Smoothened. *Front Genet* **10**, 556 (2019).

9.   Crompton, T., Outram, S.V. & Hager-Theodorides, A.L. Sonic hedgehog signalling in T-cell development and activation. *Nat Rev Immunol* **7**, 726-735 (2007).

10.   de la Roche, M. *et al.* Hedgehog signaling controls T cell killing at the immunological synapse. *Science* **342**, 1247-1250 (2013).

11.   Rovida, E. & Stecca, B. Mitogen-activated protein kinases and Hedgehog-GLI signaling in cancer: A crosstalk providing therapeutic opportunities? *Semin Cancer Biol* **35**, 154-167 (2015).

12.   Omilusik, K. *et al.* The Ca(v)1.4 calcium channel is a critical regulator of T cell receptor signaling and naive T cell homeostasis. *Immunity* **35**, 349-360 (2011).

13. Jha, M.K. *et al.* Defective survival of naive CD8+ T lymphocytes in the absence of the beta3 regulatory subunit of voltage-gated calcium channels. *Nat Immunol* **10**, 1275-1282 (2009).

14. Park, H.L. *et al.* Mouse Gli1 mutants are viable but have defects in SHH signaling in combination with a Gli2 mutation. *Development* **127**, 1593-1605 (2000).

15. Brownlie, R.J. & Zamoyska, R. T cell receptor signalling networks: branched, diversified and bounded. *Nat Rev Immunol* **13**, 257-269 (2013).

16. Aramburu, J. *et al.* Affinity-driven peptide selection of an NFAT inhibitor more selective than cyclosporin A. *Science* **285**, 2129-2133 (1999).

17. Brockman, J.A. *et al.* Coupling of a signal response domain in I kappa B alpha to multiple pathways for NF-kappa B activation. *Mol Cell Biol* **15**, 2809-2818 (1995).

18. Adachi, K. & Davis, M.M. T-cell receptor ligation induces distinct signaling pathways in naive vs. antigen-experienced T cells. *Proc Natl Acad Sci U S A* **108**, 1549-1554 (2011).

19. Kurachi, M. *et al.* The transcription factor BATF operates as an essential differentiation checkpoint in early effector CD8+ T cells. *Nat Immunol* **15**, 373-383 (2014).

20. Roychoudhuri, R. *et al.* BACH2 regulates CD8(+) T cell differentiation by controlling access of AP-1 factors to enhancers. *Nat Immunol* **17**, 851-860 (2016).

21. Samten, B. *et al.* CREB, ATF, and AP-1 transcription factors regulate IFN-gamma secretion by human T cells in response to mycobacterial antigen. *J Immunol* **181**, 2056-2064 (2008).

22. McLellan, J.S. *et al.* The mode of Hedgehog binding to Ihog homologues is not conserved across different phyla. *Nature* **455**, 979-983 (2008).

23. Trebak, M. & Kinet, J.P. Calcium signalling in T cells. *Nat Rev Immunol* **19**, 154-169 (2019).

24. Badou, A., Jha, M.K., Matza, D. & Flavell, R.A. Emerging roles of L-type voltage-gated and other calcium channels in T lymphocytes. *Front Immunol* **4**, 243 (2013).

25. Samuel, M.A. *et al.* LKB1 and AMPK regulate synaptic remodeling in old age. *Nat Neurosci* **17**, 1190-1197 (2014).

26. Bannard, O., Kraman, M. & Fearon, D.T. Secondary replicative function of CD8+ T cells that had developed an effector phenotype. *Science* **323**, 505-509 (2009).

27. Xie, J. *et al.* Activating Smoothened mutations in sporadic basal-cell carcinoma. *Nature* **391**, 90-92 (1998).

815

28.   Splawski, I. *et al.* Ca(V)1.2 calcium channel dysfunction causes a multisystem disorder including arrhythmia and autism. *Cell* **119**, 19-31 (2004).

29.   Ahmed, H., Akbari, H., Emami, A. & Akbari, M.R. Genetic Overview of Syndactyly and
820   Polydactyly. *Plast Reconstr Surg Glob Open* **5**, e1549 (2017).

30.   Atsuta, Y., Tomizawa, R.R., Levin, M. & Tabin, C.J. L-type voltage-gated Ca(2+) channel CaV1.2 regulates chondrogenesis during limb development. *Proc Natl Acad Sci U S A* **116**, 21592-21601 (2019).

825

31.   St-Jacques, B., Hammerschmidt, M. & McMahon, A.P. Indian hedgehog signaling regulates proliferation and differentiation of chondrocytes and is essential for bone formation. *Genes Dev* **13**, 2072-2086 (1999).

830   32.   Halle, S. *et al.* In Vivo Killing Capacity of Cytotoxic T Cells Is Limited and Involves Dynamic Interactions and T Cell Cooperativity. *Immunity* **44**, 233-245 (2016).

33.   Hui, C.C. & Angers, S. Gli proteins in development and disease. *Annu Rev Cell Dev Biol* **27**, 513-537 (2011).

835

34.   Badou, A. *et al.* Critical role for the beta regulatory subunits of Cav channels in T lymphocyte function. *Proc Natl Acad Sci U S A* **103**, 15529-15534 (2006).

35.   Strauss, O., Mergler, S. & Wiederholt, M. Regulation of L-type calcium channels by
840   protein tyrosine kinase and protein kinase C in cultured rat and human retinal pigment epithelial cells. *FASEB J* **11**, 859-867 (1997).

36.   Robert, V., Triffaux, E., Savignac, M. & Pelletier, L. Singularities of calcium signaling in effector T-lymphocytes. *Biochim Biophys Acta* **1833**, 1595-1602 (2013).

845

37.   Maloverjan, A., Piirsoo, M., Michelson, P., Kogerman, P. & Osterlund, T. Identification of a novel serine/threonine kinase ULK3 as a positive regulator of Hedgehog pathway. *Exp Cell Res* **316**, 627-637 (2010).

850   38.   Infante, P., Alfonsi, R., Botta, B., Mori, M. & Di Marcotullio, L. Targeting GLI factors to inhibit the Hedgehog pathway. *Trends Pharmacol Sci* **36**, 547-558 (2015).

39.   Brownell, I., Guevara, E., Bai, C.B., Loomis, C.A. & Joyner, A.L. Nerve-derived sonic hedgehog defines a niche for hair follicle stem cells capable of becoming epidermal stem
855   cells. *Cell Stem Cell* **8**, 552-565 (2011).

40.   Zitt, C. *et al.* Potent inhibition of Ca2+ release-activated Ca2+ channels and T-lymphocyte activation by the pyrazole derivative BTP2. *J Biol Chem* **279**, 12427-12437 (2004).

860   41.   Sanchez, E., Liu, X. & Huse, M. Actin clearance promotes polarized dynein accumulation at the immunological synapse. *PLoS One* **14**, e0210377 (2019).

        42.   Woehrle, T. *et al.* Pannexin-1 hemichannel-mediated ATP release together with P2X1 and P2X4 receptors regulate T-cell activation at the immune synapse. *Blood* **116**, 3475-3484
865   (2010).

        43.   Bertin, S. *et al.* The ion channel TRPV1 regulates the activation and proinflammatory properties of CD4(+) T cells. *Nat Immunol* **15**, 1055-1063 (2014).

870   44.   Sahoo, S.S. *et al.* Transient receptor potential ankyrin1 channel is endogenously expressed in T cells and is involved in immune functions. *Biosci Rep* **39** (2019).

        45.   Kotturi, M.F., Carlow, D.A., Lee, J.C., Ziltener, H.J. & Jefferies, W.A. Identification and functional characterization of voltage-dependent calcium channels in T lymphocytes. *J*
875   *Biol Chem* **278**, 46949-46960 (2003).

        46.   Schmittgen, T.D. & Livak, K.J. Analyzing real-time PCR data by the comparative C(T) method. *Nat Protoc* **3**, 1101-1108 (2008).

880   47.   Robinson, J.T. *et al.* Integrative genomics viewer. *Nat Biotechnol* **29**, 24-26 (2011).

885

890

895
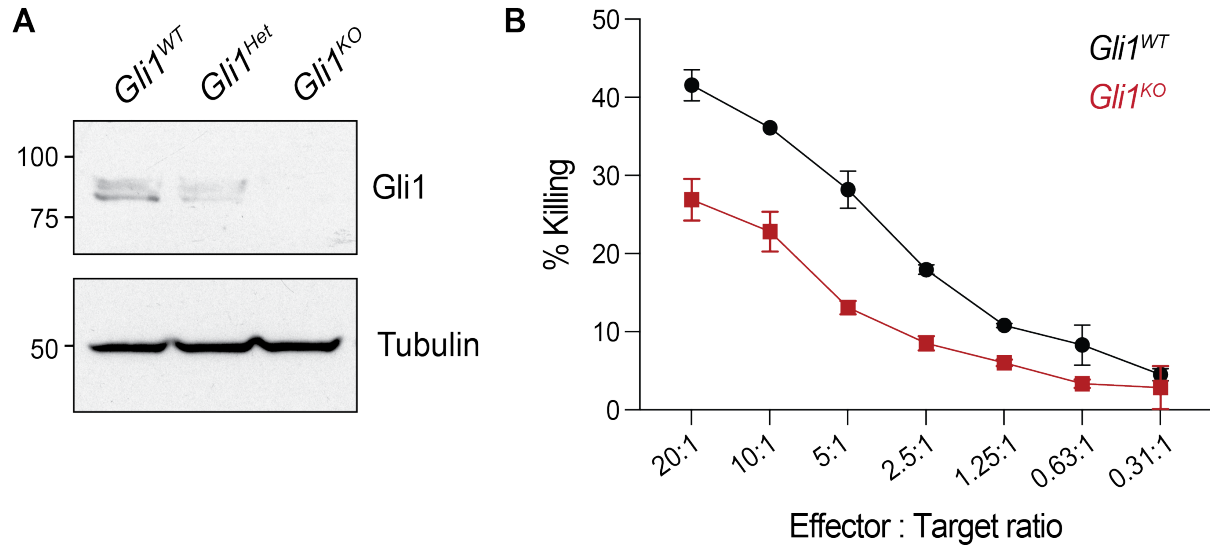
900

Figure 1: Loss of *Gli1* diminishes CTL killing.
(**A**) CTLs were generated from *Gli1^WT^*, *Gli1^Het^* and *Gli1^KO^* mice and restimulated on day 10 with plate-bound anti-CD3 antibodies for 24h. Cells were lysed and lysates blotted for protein expression of Gli1 and tubulin. n=2 independent experiments. Molecular masses are shown in kilodaltons. (**B**) On day 7 post stimulation CTLs from *Gli1^WT^* and *Gli1^KO^* mice were co-cultured with ovalbumin-pulsed EL-4 target cells for 4 hours at the indicated effector to target ratios and subjected to an LDH cytotoxicity assay. Representative data of n=3 independent experiments. Error bars indicate SD.

910

Figure 2

915

34
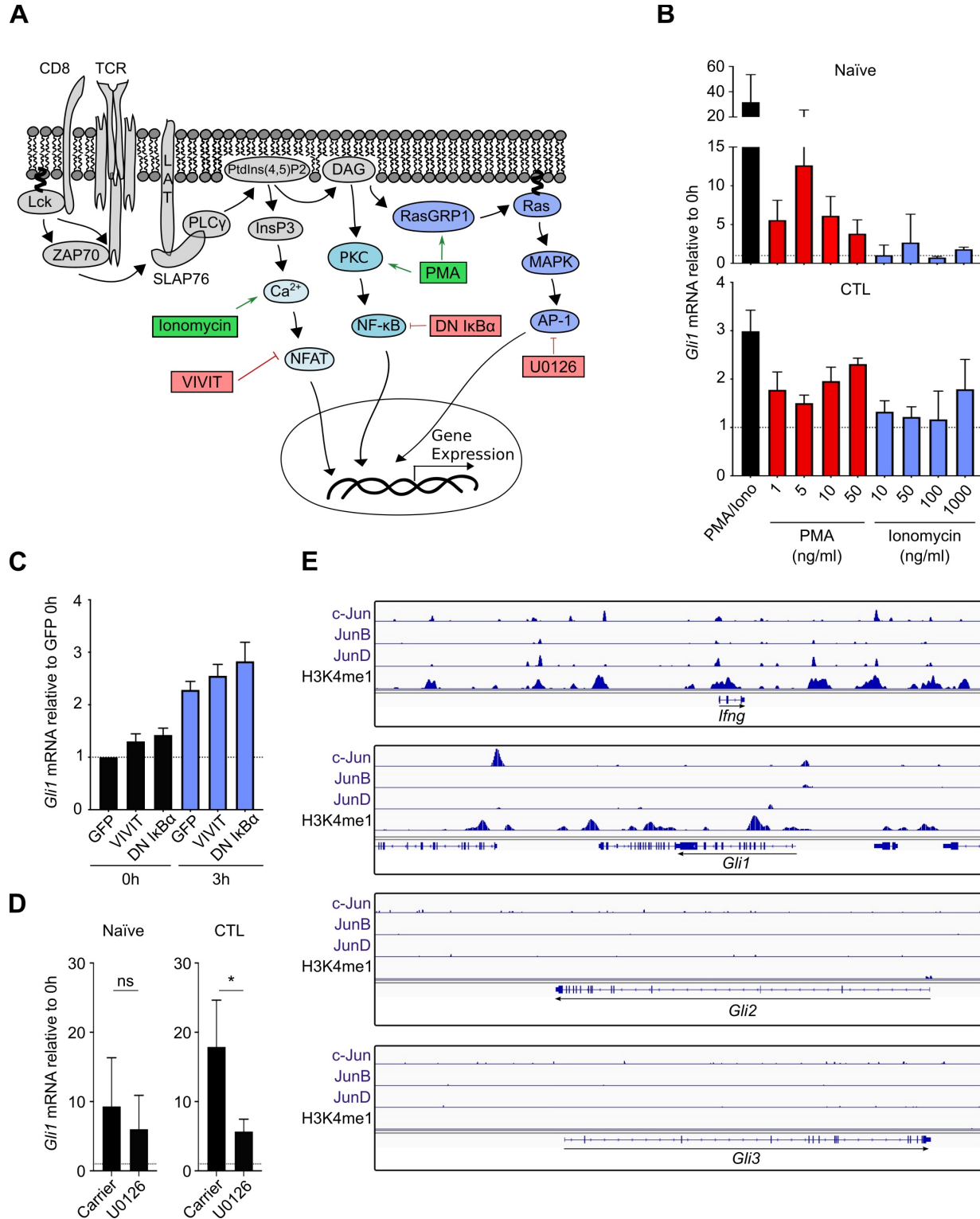
Figure 2: MAPK signalling drives Gli1 induction in CTLs post TCR stimulation.
(**A**) Schematic overview of signalling downstream of the TCR culminating in the activation of transcription factors NFAT, NF-κB and AP-1. Small molecule agonists (green) as well as antagonists and dominant negative constructs (red) of the branches of TCR signalling are shown. (**B-D**) CD8$^+$ T cells were isolated from spleens and inguinal lymph nodes of Rag2$^{-/-}$ OT-I mice. (**B**) Naïve CD8$^+$ T cells or CTLs were treated with indicated doses of PMA and/or Ionomycin for 3 hours (naïve, top panel) (CTL, bottom panel) before being subjected to qRT-PCR analysis. For double treatment with PMA and Ionomycin, 50ng/ml PMA and 1µg/ml Ionomycin was used. n=3 independent experiments. (**C**) CTLs were nucleofected with GFP, GFP-VIVIT or Dominant Negative IκBα (DN IκBα) on day 6. Cells were restimulated with anti-CD3 on day 7 for 3 hours for qRT-PCR analysis. n=3 independent experiments. (**D**) Naïve CD8$^+$ T cells were stimulated for 6h with plate-bound anti-CD3/CD28 antibodies in the presence of 10µM U0126 or carrier control (left). CTLs were restimulated for 15h with plate-bound anti-CD3 in the presence of 10µM U0126 or carrier control (right) before RNA was extracted for qRT-PCR analysis. n=3 independent experiments. (B-D) Data is normalized to *CD3ε* as a reference gene. Similar results were obtained when *Tbp* was used as a reference gene. Error bars indicate SD. p values were calculated using an unpaired two-tailed Student's t test. * indicates p<0.05. (**E**) Analysis of ChIP-Seq data from (*Kurachi et al.*) showing binding of AP-1 family members (c-Jun, JunB, JunD) at the *Gli1* promoter. Binding at the *Ifng* promoter serves as a positive control and no binding at the *Gli2* and *Gli3* promoters serve as negative controls.
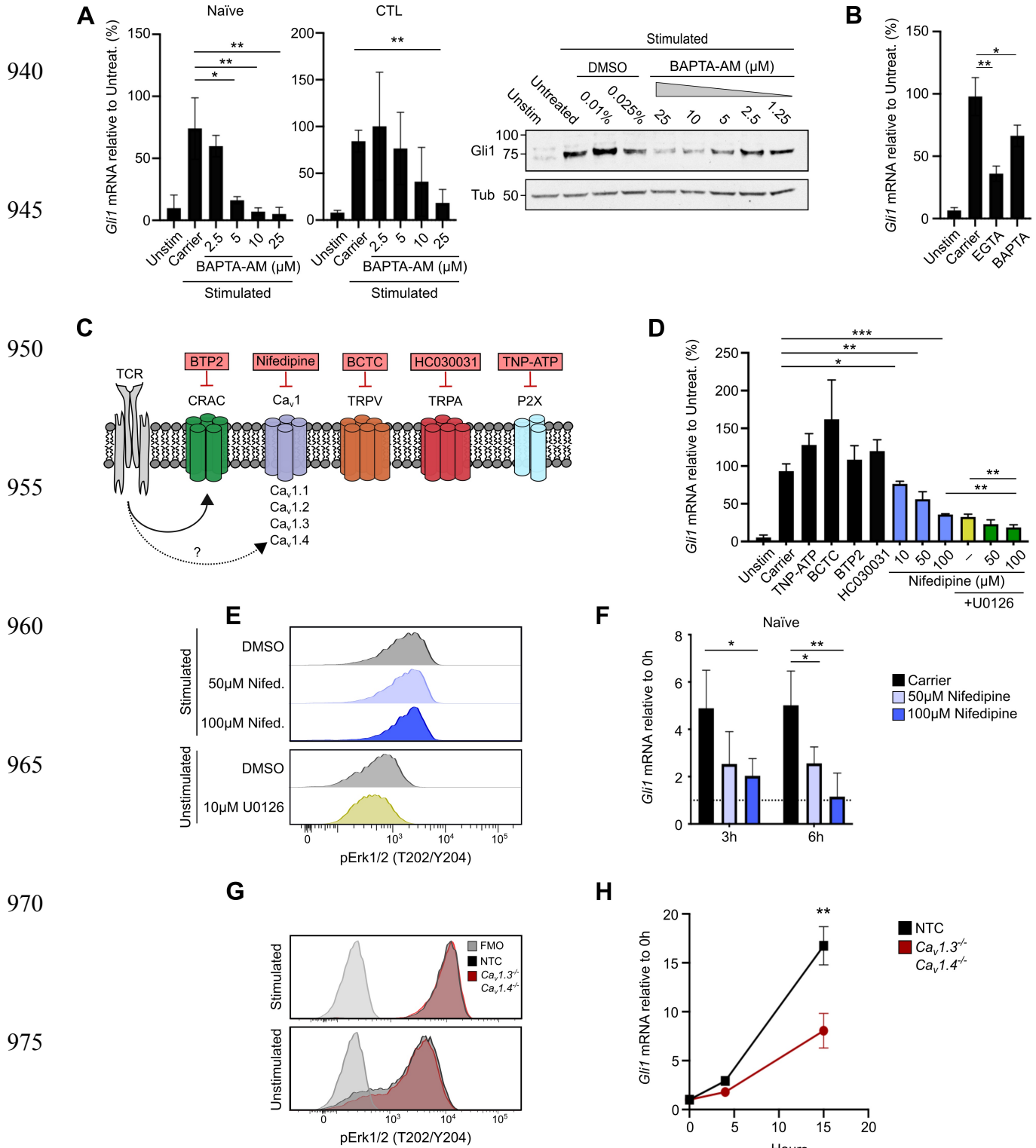
920

925

930

935

Figure 3

Figure 3: Nifedipine-sensitive Ca^{2+} channels control Gli1 induction in naïve CD8$^+$ T cells and CTLs post TCR stimulation.

(**A**) Naïve CD8$^+$ T cells (left panel) or CTLs (middle panel) were stimulated with plate-bound anti-CD3/CD28 or anti-CD3 antibodies alone for 3 hours in the presence of indicated doses of the cell permeable Ca^{2+} chelator BAPTA-AM or carrier control. RNA was extracted for qRT-PCR analysis. Immunoblot analysis of Gli1 and tubulin of CTLs left unstimulated or restimulated with plate-bound anti-CD3 for 3 hours in the presence of BAPTA-AM or carrier control is shown (right panel). Molecular masses are shown in kilodaltons. n=3 independent experiments. (**B**) CTLs were restimulated for 3h with plate-bound anti-CD3 in the presence of 1.25mM BAPTA, 1.25mM EGTA or carrier control before RNA was extracted for qRT-PCR analysis (right panel). n=3 independent experiments. (**C**) Schematic overview of Ca^{2+} channels with respective antagonists (red) used in this study. (**D**) CTLs were restimulated with plate-bound anti-CD3 in the presence of the indicated inhibitors or carrier control for 15h before RNA was extracted for qRT-PCR analysis. n=3-4 independent experiments. (**E**) CTLs were restimulated with 10µg/ml cross-linked soluble anti-CD3 in the presence of Nifedipine, 10µM U0126 or carrier control. Cells were subsequently prepared for intracellular flow cytometric analysis. n=2 independent experiments. (**F**) Naïve CD8$^+$ T cells were stimulated with plate-bound anti-CD3ε in the presence of the indicated doses of Nifedipine or carrier control. n=3 independent experiments. (**G, H**) Activated CD8$^+$ T cells were electroporated with RNP complexes at day 2 post stimulation to generate $Ca_v1.3/1.4^{-/-}$ (KO) or non-targeting control (NTC) CTLs. CTLs were restimulated on day 8/9 with 10µg/ml cross-linked soluble anti-$CD3\varepsilon$ for flow cytometric analysis of pErk (**G**) or restimulated with plate-bound anti-CD3 for qRT-PCR analysis (**H**). n=3 independent experiments. (A,B,D,F,H) Data is normalized to $CD3\varepsilon$ as a reference gene. Similar results were obtained when Tbp was used as a reference gene. Error bars indicate SD. p values were calculated using an unpaired two-tailed Student's t test (A,B,D,F) or two-way ANOVA (H) and * indicates p<0.05, ** p<0.01, and *** p<0.001.
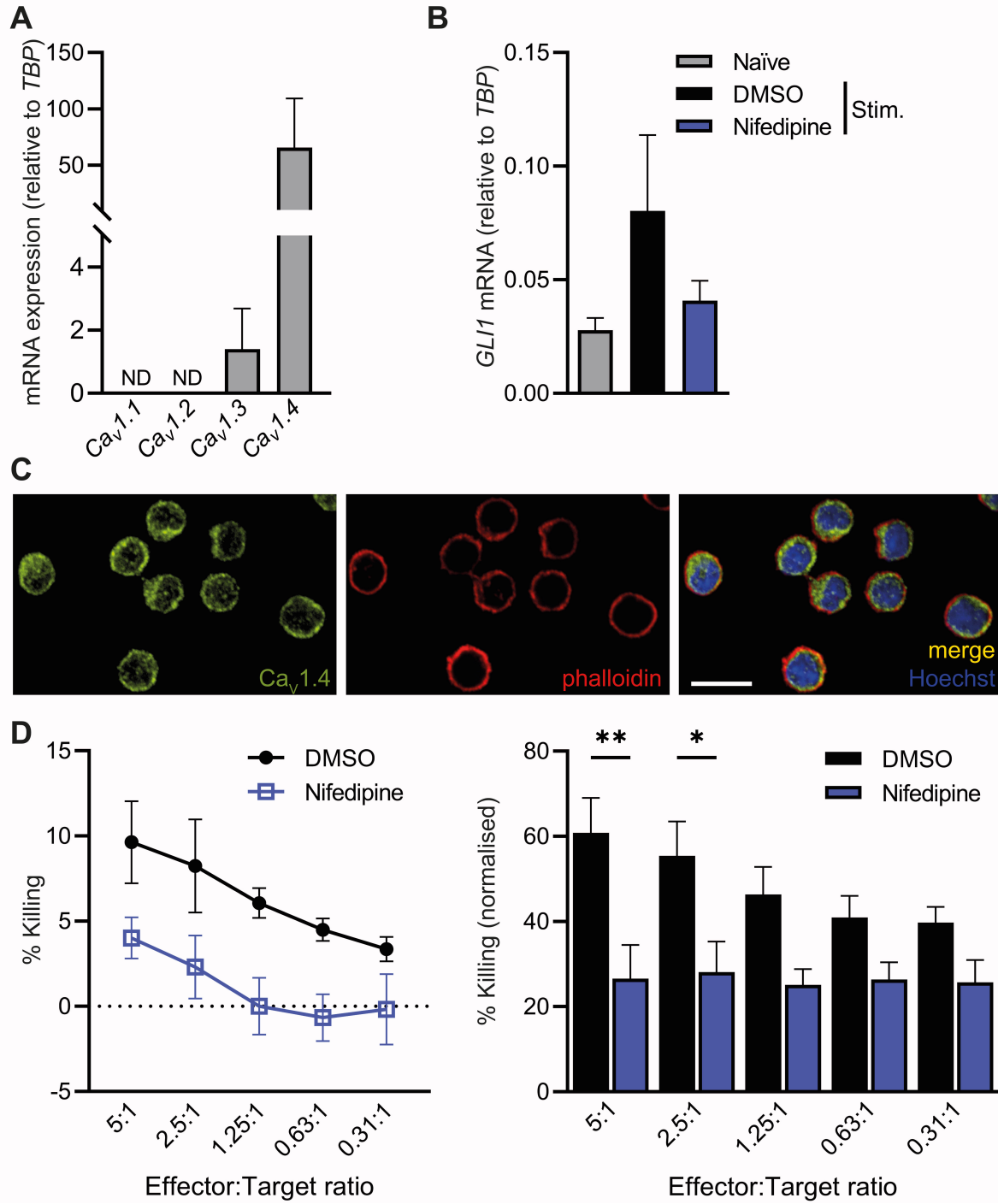
1015

1020

Figure 4

Figure 4: Ca$_v$1 family channels are responsible for Gli1 induction and control killing in human CTLs.

Naïve human CD8$^+$ T cells were isolated from peripheral blood of healthy donors. (**A**) Cells were processed for qRT-PCR analysis of human Ca$_v$1.1 (*CACNA1S*), Ca$_v$1.2 (*CACNA1C*), Ca$_v$1.3 (*CACNA1D*) and Ca$_v$1.4 (*CACNA1F*) channel expression. Values were normalized to *TBP* as a reference gene. ND: Not Detected. Error bars indicate SEM. n=7 donors. (**B**) RNA was extracted before and after stimulation with human T-activator CD3/CD28 beads for 2 days in the presence of 100 μM nifedipine or DMSO (carrier control). Error bars indicate SEM. n=11 donors. (**C**) T cells were stimulated with human T-activator CD3/CD28 beads for 3 days. On d11, CTLs were stained with antibodies against Ca$_v$1.4, phalloidin and Hoechst. Scale bar=10 μm. n=8 donors, representative donor shown. (**D**) T cells were stimulated with human T-activator CD3/CD28 beads for 3 days and again restimulated with T-activator CD3/CD28 beads on d10 for 3 days. On d14-d15, CD8$^+$ T cells were co-cultured with P815 target cells at indicated effector to target ratios and subjected to an LDH cytotoxicity assay in the presence of 100μM Nifedipine or DMSO (carrier control). Left panel: Error bars indicate SD, representative donor shown. Right panel: Error bars indicate SEM, n=6 donors. p values were calculated using two-way ANOVA. * indicates $p < 0.05$, and ** $p < 0.01$.

39
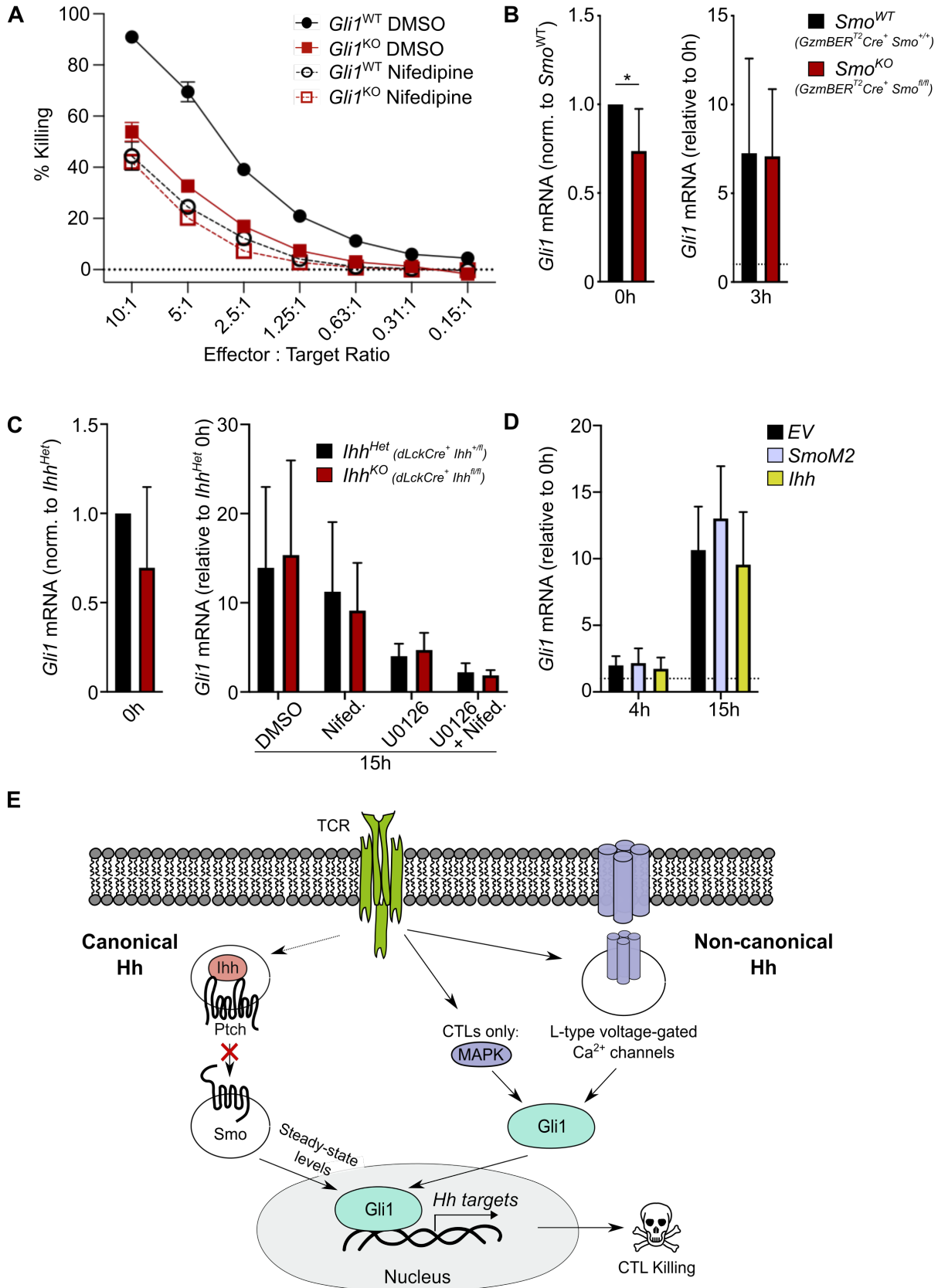
Figure 5

Figure 5: Ca$_v$1 family channels control CTL killing in a Gli1-dependent manner and function independently of canonical Hh signaling.

(**A**) CTLs were generated from *Gli1^{WT}*, *Gli1^{Het}* and *Gli1^{KO}* mice. On day 7, cells were co-cultured with either peptide-pulsed EL-4 cells (OTI) or anti-CD3 antibody-coated P815 target cells at the indicated effector to target ratios and subjected to an LDH cytotoxicity assay in the presence of 100µM Nifedipine or carrier control. Error bars indicate SD. Representative of n=4 independent experiments. (**B**) CTL were generated from *GzmBERTCre$^+$ Smo$^{+/+}$* (*Smo^{WT}*) or *GzmBERTCre$^+$ Smo$^{fl/fl}$* (*Smo^{KO}*) mice. Cells were treated with 4-OH-Tamoxifen for the duration of the *in vitro* experiments. CTLs were restimulated for 3h on day 8/9 for qRT-PCR analysis. n=5 mice per condition, 5 independent experiments. (**C**) CD8$^+$ T cells were isolated from *dLckCre$^+$ Ihh$^{fl/+}$* (*Ihh^{Het}*) or *dLckCre$^+$ Ihh$^{fl/fl}$* (*Ihh^{KO}*) mice. CTLs were restimulated for 15h on day 8/9 in the presence of 100µM Nifedipine and/or 10µM U0126 or carrier control for qRT-PCR analysis. n=5 (naïve) and n=3 (restimulation) independent experiments. (**D**) CD8$^+$ T cells were retrovirally transduced with pMig constructs encoding empty vector (EV), SmoM2 or Ihh, respectively. Sorted, transduced CTLs were restimulated on day 8/9 for qRT-PCR analysis. n=3 mice per condition, 3 independent experiments. (B-D) Data is normalized to *CD3ε* as a reference gene. Similar results were obtained when *Tbp* was used as a reference gene. Error bars indicate SD. No statistically significant differences were observed. (**E**) Model of TCR-induced Gli1 induction: two arms of Hedgehog (Hh) signaling are induced post-TCR stimulation. Canonical Hh signaling is initiated by binding of intracellular Ihh to Ptch, which results in activation of Smo. Smo is the key signal transducer of canonical Hh signalling and was previously shown to regulate steady-state Gli1 protein expression (*de la Roche et al*). TCR stimulation also activates Ca$_v$ channels and we show here that these Ca$_v$ channels are critical to induce Gli1 transcription either independently (naïve CD8$^+$ T cells) or in conjunction with MAPK signalling (CTLs). The TCR-induced Gli1 activation is essential for efficient CTL killing.